HYGROEXPANSION-CREEP MODEL FOR CORRUGATED FIBERBOARD[1]

Thomas J. Urbanik

Research Engineer
USDA Forest Service
Forest Products Laboratory
One Gifford Pinchot Drive
Madison, WI 53705-2398

(Received July 1994)

ABSTRACT

A model was developed for characterizing the creep response of corrugated fiberboard subjected to constant compression load and sinusoidally varying relative humidity. Separate hygroexpansion and mechanosorptive components of deformation during the primary and secondary phases of creep are characterized in terms of six parameters, A_0, A, θ, τ, μ_1, and μ_2. Parameters A_0 and A are the magnitude and amplitude levels, respectively, of a sinusoidal hygroexpansion response, and θ is the corresponding phase lag relative to relative humidity. The model makes mechanosorption a function of hygroexpansion and predicts an instantaneous creep rate that varies with the rate of hygroexpansion. An average creep rate of mechanosorption decreases from a value that initiates primary creep to a steady-state value throughout secondary creep. The change occurs exponentially with a time-constant τ. Creep constants μ_1 and μ_2 are proportional to the initial and secondary creep rates, respectively. The model provides a way to characterize cyclic creep data.

Keywords: Compression strength, constant load test, creep rate, cyclic humidity, duration of load, long-term test.

INTRODUCTION

When cellulosic materials are subjected to stress and relative humidity (RH), they increasingly deform (creep) and can eventually collapse or rupture. The mechanisms of creep and failure are not well understood. Researchers have applied various spring-dashpot analogies to characterize the viscoelastic, hygrothermal, and mechanosorptive effects. Essentially, viscoelastic creep is caused by stress and the time required for deformation to respond to stress. Hygrothermal phenomena make viscoelastic effects a function of moisture and temperature. Mechanosorption is a cumulative ratcheting of deformation following each change in material moisture content.

In the compressive creep response of paper, mechanosorption has been found to be the most serious of the creep mechanisms. Byrd and Koning (1978) found that creep rates of corrugated fiberboard specimens were 3 to 14 times greater during cyclic 35% to 90% RH than during constant 90% RH. In compression tests of corrugated boxes (Leake and Wojcik 1992), specimens survived only 3 to 15 days when subjected to cyclic 50% to 90% RH, compared to 55 days when subjected to constant 90% RH. During the cyclic tests, the cumulative exposures to the high RH portion of the cycles were less than the continuous exposures during the constant RH. Consequently, the contribution of viscoelastic and hygrothermal mechanisms during cyclic creep was reduced.

Hygroexpansion is the swelling and shrinking that occurs with RH changes. Cyclic creep data exhibit hygroexpansion superimposed on the mechanosorptive creep. Researchers have tried to separate these two forms. Haslach et

[1] The Forest Products Laboratory is maintained in cooperation with the University of Wisconsin. This article was written and prepared by U.S. Government employees on official time, and it is therefore in the public domain and not subject to copyright.

Wood and Fiber Science, 27(2), 1995, pp. 134–140

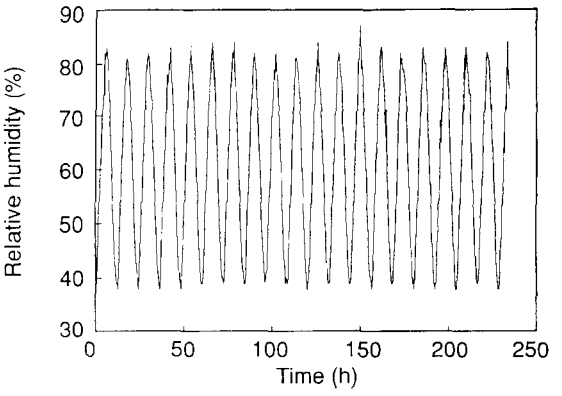

FIG. 1. Relative humidity varying with time and following a sinusoidal control signal with B_0 = 66% RH, B = 21% RH, $\phi = -\pi/2$, and P = 12 h.

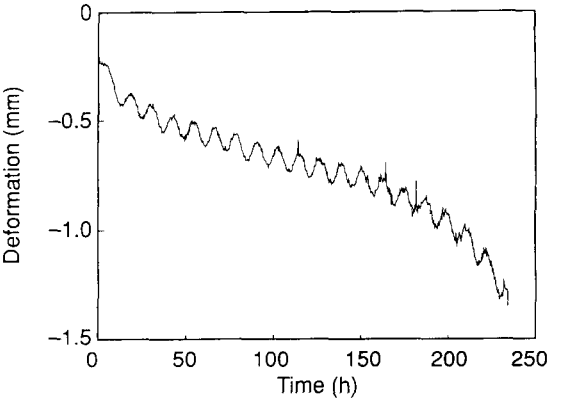

FIG. 2. Deformation varying with time of a short column of corrugated fiberboard subjected to 1.75 kN/m (10 lbf/in.) static edgewise compression and cyclic relative humidity (Fig. 1). The short column was 51 mm (2 in.) wide by 38 mm (1.5 in.) high, with height in the axis direction of the flutes. The region of secondary creep lies approximately between 50 h and 150 h.

al. (1991) proposed various loads and RH rate changes to separate the swelling and creep components of tension data on paper. Their procedure was complicated by the primary creep following the load application and was not successfully generalized. Soremark and Fellers (1993) conducted bending tests of steel-backed corrugated fiberboard strips with and without a load during cyclic RH. Hygroexpansion prior to loading was used to predict the hygroexpansion during creep. Such a procedure is sensitive to the repeatability of successive RH cycles.

Fridley et al. (1992) proposed a mechanosorptive model that yielded a strain rate of wood beams in bending proportional to a nondirectional rate of change of a relative moisture content. However, data were insufficient to predict either the form of the moisture function or the experimental RH profile. However, data from Uesaka et al. (1992) demonstrated a linear relation between hygroexpansion strain and moisture content of paper. Thus, Fridley's model seems applicable to paper if the form of a hygroexpansion function could be extracted from creep data and used in place of the moisture function. Tests of corrugated fiberboard at the Forest Products Laboratory (FPL) (Laufenberg and Gunderson 1994) yielded mathematically describable creep data following an accurate sinusoidal RH profile and are ideal for testing Fridley's model.

MECHANOSORPTIVE CREEP MODEL

Relative humidity in the FPL test chamber can be made to follow the form of a sinusoidal control signal Y(t) specified by

$$Y(t) = B_0 + B \sin(\omega t + \phi) \qquad (1)$$

to yield RH that cycles during time t at a frequency ω with an amplitude B superimposed on a steady-state magnitude B_0 and is initially offset by a phase angle ϕ. Figure 1 shows typical RH data from a test schedule in which the cycle period P given by $P = 2\pi/\omega$ was 12 h. The deformation of a short-column specimen of nominal C-flute corrugated fiberboard subjected to static edgewise compression and cyclic RH is shown in Fig. 2.

The deformation function X(t) is the sum of a hygroexpansion function $X_h(t)$ caused by moisture content and a mechanosorptive creep function $X_c(t)$ caused by the cumulative ratcheting of swelling and shrinking effects with each change in specimen moisture content. Hygroexpansion of unloaded specimens was ob-

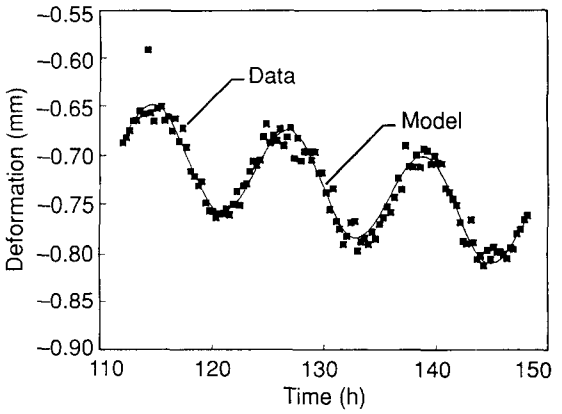

FIG. 3. Comparison between a hygroexpansion creep model given by Eq. (9) and a subset of deformation data (Fig. 2) varying with time.

served to vary with the same form as RH. Therefore, the characterization considered for $X_h(t)$ is

$$X_h(t) = A_0 + A \sin \alpha \qquad (2)$$

where A_0 and A are respective magnitude and amplitude levels and α is defined as

$$\alpha = \omega t + \phi - \theta \qquad (3)$$

with θ being the phase lag of X_h relative to RH. The rate of hygroexpansion is predictable by differentiating Eq. (2) with respect to time to obtain

$$\frac{dX_h}{dt} = A\omega \cos \alpha. \qquad (4)$$

An expression for $X_c(t)$ can be obtained from dX_h/dt by first equating the creep rate R to dX_c/dt. Fridley et al. (1992) characterized the creep rate of mechanosorption as being proportional to the magnitude of the rate of change of a relative moisture content. Adsorption and desorption of moisture were considered to cause equal amounts of creep. Uesaka et al. (1992) observed that hygroexpansion varies linearly with moisture content. Thus, instead of moisture content change, our model uses the magnitude of the rate of hygroexpansion to predict

$$R = \frac{dX_c}{dt} = \mu \left| \frac{dX_h}{dt} \right| \qquad (5)$$

where μ is a mechanosorptive creep constant. Substituting Eqs. (3) and (4) into Eq. (5) and integrating the result with respect to t yield an expression for $X_c(t)$.

$$X_c(t) = \int_0^t R \, dt = A\omega \int_0^t \mu |\cos \alpha| \, dt. \qquad (6)$$

Case 1. Fixed μ

The expression x_c is used here for X_c when the value of μ in Eq. (6) is assumed to remain constant during a short time interval $t_1 \le t \le t_2$. Solving Eq. (6) for the case of a fixed μ yields the creep function

$$x_c(t) = A\mu[C_i(t)]_{t_1}^{t_2} + X_0; \qquad t_1 \le t \le t_2 \qquad (7)$$

where

$$C_i(t) = \sin \alpha \, \text{sign}(\cos \alpha) + \frac{2}{\pi}(\omega t - \arctan(\tan \alpha)) \qquad (8)$$

and X_0 is the creep deformation at time t_1. The "sign" function in Eq. (8) is used to yield the value ± 1. Therefore, if μ is constant, X(t) is predicted by

$$X(t) = X_h(t) + x_c(t) \qquad (9)$$

in which X_h is given by Eq. (2) and x_c is given by Eq. (7). A comparison between Eq. (9) and data is shown in Fig. 3. The data (Fig. 3) around time t = 130 h are a three-cycle subset of the continuous data (Fig. 2) up to failure. Values of $A_0 + X_0$, A, θ, and μ were determined by fitting Eq. (9) to the data and are given in Table 1.

Figure 4 shows the X_h- and x_c-components of X(t) on separate scales to reveal how cyclic hygroexpansion causes a corresponding creep. The creep rate dx_c/dt is greatest whenever the magnitude of dX_h/dt is greatest, corresponding to $X_h = 0$ in Fig. 4. The creep rate approaches

TABLE 1. *Fit of* $X(t) = X_h(t) + x_c(t)$ *to deformation data around various times.*

Time (h)	$A_0 + X_0$ (μm)	A (μm)	θ (degrees)	μ	$\bar{R}$ (μm/hour)
30	−388	43.2	20.6	−0.309	−4.46
75	−553	48.0	20.2	−0.169	−2.70
130	−691	48.1	24.5	−0.135	−2.17
200	−869	50.4	23.2	−0.362	−6.08

zero and creep pauses whenever hygroexpansion along the X_h-curve reverses direction. It can be further observed that with each quarter-cycle of hygroexpansion, deformation creeps by an equal amount (Fig. 4). This repeatability can be used to determine an average creep rate during the undulations caused by mechanosorption. Equations (3), (7), and (8) predict that α, t, and x_c change by the amounts

$$\Delta\alpha = \frac{\pi}{2}, \qquad \Delta t = \frac{\pi}{2\omega}, \qquad \Delta x_c = A\mu \quad (10)$$

respectively, where the Δ's stand for the difference per quarter-cycle. The average creep rate $\bar{R}$ becomes

$$\bar{R} = \frac{\Delta x_c}{\Delta t} = \frac{2A\mu\omega}{\pi}. \quad (11)$$

In terms of P, the average creep rate is

$$\bar{R} = \frac{4A\mu}{P}. \quad (12)$$

Equation (11) predicts that when A and μ remain constant, $\bar{R}$ is proportional to the RH cycle frequency. Short RH cycles are predicted to be more severe than long RH cycles because more mechanosorptive events occur per interval of time. This prediction is consistent with tension creep of paper; Gunderson and Tobey (1990) found that the creep per RH cycle, for various cycles between a 20-min and a 168-h cycle period, remained constant. However, in the compression creep of corrugated boxes (Leake and Wojcik 1992), long RH cycles were more severe. Boxes survived for 15, 5, and 3 days when subjected to 12-, 24-, and 48-h RH cycle periods, respectively. Additional research is needed to determine how the

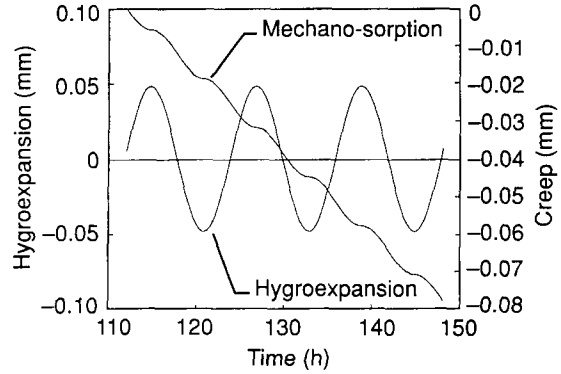

FIG. 4. Comparison over time between the hygroexpansion of a short column of corrugated fiberboard subjected to cyclic RH and the mechanosorption caused by static compression and the hygroexpansion. Hygroexpansion is plotted with $A_0 = 0$.

RH cycle frequency affects the diffusion of moisture and the creep rate when A and μ do not remain constant.

The average creep rate at t = 130 h determined by Eq. (12) is given in Table 1. For comparison with other times, the data from Fig. 2 were further characterized by repeatedly fitting Eq. (9) to a three-cycle window of data as the window was moved along the deformation curve. Values of $A_0 + X_0$, A, θ, μ, and $\bar{R}$ at various times are given in Table 1. A continuous plot of the determinations of $\bar{R}$ is shown in Fig. 5. The transitions from primary creep to secondary creep around 50 h and from secondary creep to tertiary creep around 150 h are more easily recognizable from the $\bar{R}$-plot (Fig. 5) than from the deformation data (Fig. 2). Tertiary creep leading to failure begins after 150 h.

Case 2. Variable μ

The μ-evaluations in Table 1 do not remain fixed. Equation (12) predicts that if A and P remain constant, the variation of $\bar{R}$ results from μ. In the moving window data (Fig. 5), $\bar{R}$ up to 150 h varied empirically from an initial creep rate R_1 at t = 0 to a steady-state creep rate R_2 approached during secondary creep. The change occurred exponentially with t according to the function

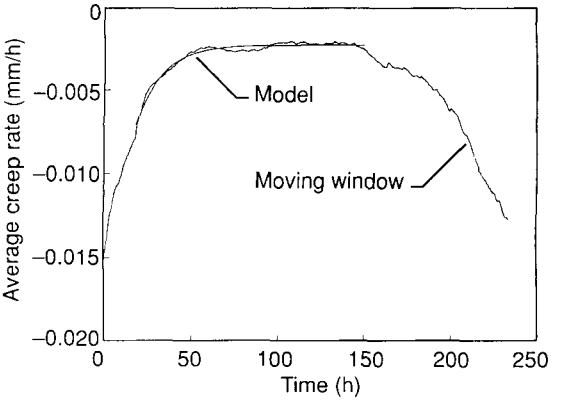

FIG. 5. Comparison over time between evaluations of average creep rate $\bar{R}$ by a moving window fit of Eq. (9) to deformation varying with time data (Fig. 2) and Eq. (13) fit to the $\bar{R}$-evaluations.

$$\bar{R}(t) = R_2 + (R_1 - R_2)e^{-t/\tau} \qquad (13)$$

in which τ is a time-constant. Equation (13) describes the response of a general first-order system subjected to a step input equal to $R_2 - R_1$. The response of such a system is 63.2%, 95.0%, and 99.3% completed after 1, 3, and 5 time-constants, respectively. Value of R_1, R_2, and τ, determined by fitting Eq. (13) to the moving window $\bar{R}$-evaluations spanning three full cycles between 18 and 150 h are as follows:

Time (h)	R_1 (μm/h)	R_2 (μm/h)	τ (h)
18–150	−18.4	−2.26	15.2

A plot of $\bar{R}(t)$ during primary and secondary creep by Eq. (13) is superimposed upon the plot of $\bar{R}$ by the moving window fit by Eq. (9) (Fig. 5). Equation (13) was found to accurately characterize the $\bar{R}$-response of a large number of cases of paper, corrugated fiberboard, and corrugated tube cyclic creep data.

Equation (12) predicts that the variation of μ with t will have the same form as $\bar{R}(t)$. Therefore, a function for $\mu(t)$ during primary and secondary creep is predicted to be

$$\mu(t) = \mu_2 + (\mu_1 - \mu_2)e^{-t/\tau} \qquad (14)$$

in which the initial creep constant μ_1 and the steady-state creep constant μ_2 are determined from Eq. (12) according to

$$\mu_1 = \frac{PR_1}{4A}, \qquad \mu_2 = \frac{PR_2}{4A}. \qquad (15)$$

Substituting Eq. (14) into Eq. (6) and solving the integral yield our model for deformation during primary and secondary creep is

$$X_c(t) = A\mu_2[C_i(t)]_0^t + \\ + A\omega(\mu_1 - \mu_2)\int_0^t F(t)\,dt \qquad (16)$$

in which $C_i(t)$ is given by Eq. (8) and the function F(t) is given by

$$F(t) = e^{-t/\tau}|\cos\alpha| \qquad (17)$$

The form of F(t) is plotted in Fig. 6. The function can be integrated between arbitrary limits of time for use in Eq. (16) by summing the components of integration between roots. For values of $t \geq 0$, the roots to Eq. (17) are

$$r_n = \frac{n\pi + 2(\theta - \phi)}{2\omega}; \qquad n = 0, \pm1, \pm2 \ldots;$$

$$n \geq \frac{2(\phi - \theta)}{\pi}. \qquad (18)$$

Function F(t) can thus be integrated by dividing the interval from 0 to t into subintervals between roots and using the formula

$$\int_{t_i}^{t_j} F(t)\,dt = \left|\frac{\tau e^{-t/\tau}(\omega t \sin\alpha - \cos\alpha)}{(\omega\tau)^2 + 1}\right|_{t_i}^{t_j};$$

$$t_i \geq r_n; \qquad t_j \leq r_{n+1}. \qquad (19)$$

From the above results, our model for deformation during primary and secondary creep is predicted by

$$X(t) = X_h(t) + X_c(t) \qquad (20)$$

in which X_h is given by Eq. (2) and X_c is given by Eq. (16). Values of A_0, A, θ, μ_1, μ_2, and τ were determined by fitting Eq. (20) to the previous data (Fig. 2) up to 150 h:

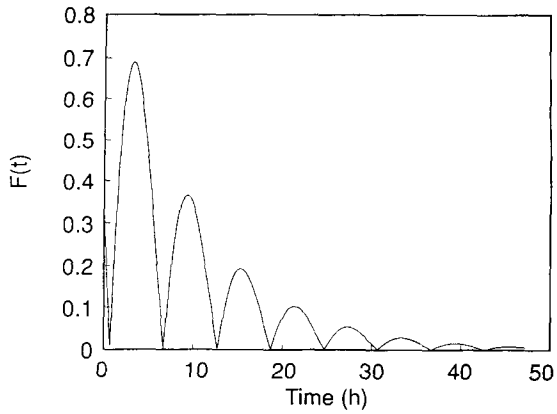

FIG. 6. Plot of F(t) showing that the function can be integrated by summing the components of integration between roots. Inputs to F(t) were taken from the Eq. (20) fit.

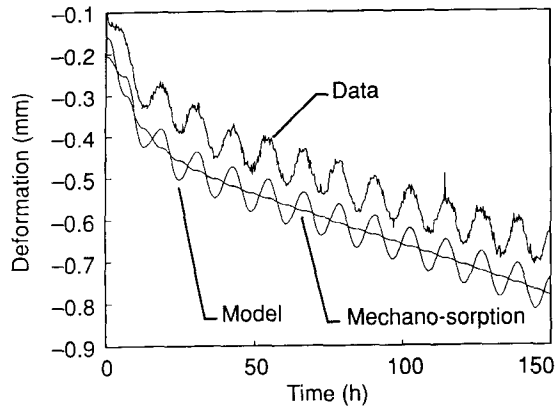

FIG. 7. Comparison between subset of deformation varying with time data (Fig. 2) and plot of Eq. (20) fit to the data. Vertical scale of deformation data is offset for clarity.

Time (h)	A_0 (μm)	A (μm)	θ (degrees)	μ_1	μ_2	τ (h)	R_1 (μm/h)	R_2 (μm/h)
0–150	−154	45.8	20.8	−2.15	−0.159	9.25	−32.9	−2.42

The creep rates R_1 and R_2 were determined from μ_1 and μ_2, respectively, using Eq. (12). A comparison between Eq. (20) and the deformation data is shown in Fig. 7.

A prediction of the average creep $\bar{X}_c$, free of the undulations caused by cyclic mechanoadsorption, can be useful when fitting Eq. (20) to data to characterize and compare different materials. A function for $\bar{X}_c(t)$ can be determined by integrating Eq. (13) with respect to t to obtain

$$\bar{X}_c(t) = \int_0^t \bar{R}\, dt = \tau(e^{-t/\tau} - 1)(R_2 - R_1) + R_2 t. \quad (21)$$

After A, τ, μ_1 and μ_2 are determined by Eq. (20) and R_1 and R_2 are determined using Eq. (15), Eq. (21) can be used to predict the average deformation that will occur at a critical time. The inverse problem of predicting the time corresponding to a critical deformation can also be determined. For this case, Newton's algorithm was found to work well. A plot of Eq. (21) is compared with data in Fig. (8). The point on the plot at t = 92 h is the point at which the specimen creeps to a critical deformation, assumed to be 0.5 mm.

DISCUSSION

In the above-described model for characterizing creep data from a cyclic humidity test of corrugated fiberboard, deformation caused by a static load and a sinusoidally varying RH is separated into hygroexpansion and mechanosorptive components. The model quantifies the effect of hygroexpansion on mechanosorptive creep throughout the primary and secondary phases of creep. The results are useful for comparing materials and cyclic environments.

The creep model derived from Eq. (5) accounts only for mechanosorption, albeit the most serious among mechanosorptive, viscoelastic, and hygrothermal mechanisms, but predicts that creep momentarily ceases whenever specimen hygroexpansion reverses direction. To determine if the effects of viscoelastic creep and hygrothermal creep are measurable, the creep rate model was expanded to the form

$$R = \mu \left| \frac{dX_h}{dt} \right| + \beta X_h \quad (22)$$

in which β is a constant that superimposes a creep rate varying with hygroexpansion caused

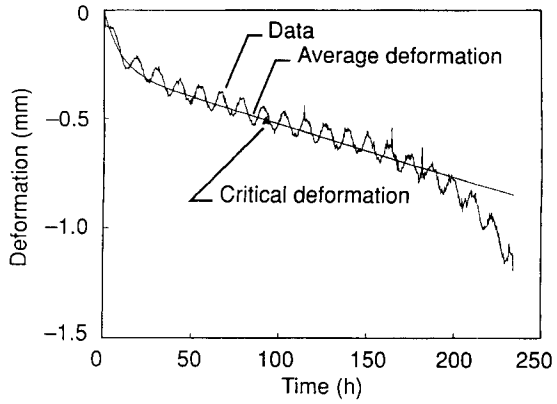

FIG. 8. Comparisons between deformation varying with time data (Fig. 2) and average deformation predicted by Eq. (21). The point on the plot of average deformation corresponds to failure time if failure is defined to be when creep exceeds 0.5 mm (0.02 in.).

by moisture content. A successful deformation function derived from Eq. (22) that could characterize multiple creep mechanisms was not found. In essence, once mechanosorption was accounted for, the noise in the data precluded an account of secondary creep mechanisms. Additional research is needed to characterize the combined effects of mechanosorptive, viscoelastic, and hygrothermal creep.

CONCLUSIONS

The objective of the study reported here was to determine if a characterization of the hygroexpansion of corrugated fiberboard subjected to cyclic RH and compression could be used to predict the mechanosorptive creep response. Corrugated fiberboard test specimens were subjected to compression and sinusoidal cyclic RH schedules. The hygroexpansion response cycled with a similar sinusoidal wave form that lagged out of phase behind the RH input. The instantaneous creep rate was proportional to the magnitude of the rate of hygroexpansion and cycled between zero and peak levels with each cycle of hygroexpansion. An average creep rate per cycle decayed exponentially from a value initiating primary creep to a steady-state value throughout secondary creep. The form of the rate decay function yielded a deformation model characterizing mechanosorptive creep. A complete model with hygroexpansion and mechanosorptive terms fit cyclic creep data during primary and secondary creep very well.

REFERENCES

BYRD, V. L., AND J. W. KONING, JR. 1978. Edgewise compression creep in cyclic relative humidity environments. TAPPI 61(6):35–37.

FRIDLEY, H. J., R. C. TANG, AND L. A. SOLTIS. 1992. Creep behavior model for structural lumber. J. Struct. Eng. 118(8):2261–2277.

GUNDERSON, D. E., AND W. E. TOBEY. 1990. Tensile creep of paperboard—Effect of humidity change rates. Pages 213–226 *in* Proceedings, Materials Interactions Relevant to the Pulp, Paper, and Wood Industries, Materials Research Society, Pittsburgh, PA.

———, AND T. L. LAUFENBERG. 1994. Apparatus for evaluating stability of corrugated board underload in cyclic humidity environment. Exp. Tech. 18(1):27–31.

HASLACH, H. W., M. G. PECHT, AND W. XIN. 1991. Variable humidity and load interaction in tensile creep of paper. Pages 219–224 *in* Proceedings, International Paper Physics Conference, TAPPI, Atlanta, GA.

LEAKE, C., AND R. WOJCIK. 1992. Humidity cycling rates: How they affect container life spans. Pages 134–144 *in* T. Laufenberg and C. Leake, eds. Proceedings, Cyclic Humidity Effects on Paperboard packaging. Forest Products Laboratory, Madison, WI.

SOREMARK, C., AND C. FELLERS. 1993. Mechanosorptive creep and hygroexpansion of corrugated board in bending. J. Pulp Paper Sci. 19(1):J19–J26.

UESAKA, T., C. MOSS, AND Y. NANRI. 1992. The characterization of hygroexpansivity of paper. J. Pulp Paper Sci. 18(1):J11–J16.